Vertical Waveguide-to-Microstrip Self-Diplexing Transition for Dual-Band Applications

Emilio Arnieri, *Member, IEEE*, Francesco Greco, *Member, IEEE*, Luigi Boccia, *Senior Member, IEEE*, and Giandomenico Amendola, *Senior Member, IEEE*

***Abstract*— This letter presents a novel vertical waveguide-to-microstrip self-diplexing transition for dual-band applications. The transition is realized with standard printed circuit board (PCB) manufacturing processing, making it suitable for mass production and practical applications. A standard waveguide is screwed on the topside of the stack-up. Dual-band self-diplexing operation is achieved by coupling two microstrips (one for each band) to two radiating patches through H-shaped slots. The operating bandwidth has been enhanced by adding two parasitic patches above the radiating ones. Metalized via holes are used to form a cage around the rectangular waveguide and the microstrips to prevent power leakage. A prototype has been fabricated to operate at K/Ka frequency band. The experimental results show a −10 dB matching bandwidth of 20% and 14% for the lower and upper bands, respectively. Within these ranges, the maximum measured insertion loss is about 0.6 and 0.7 dB, respectively.**

***Index Terms*— Dual-band, microstrip-to-waveguide transition, millimeter-wave, PCB, substrate-integrated waveguide (SIW).**

I. Introduction

RECTANGULAR metallic waveguides (RWGs) are important components in many microwave and millimeter-wave modules due to their high power handling and low insertion loss characteristics. For this reason, RWGs are widely used in satellite receivers, horn antenna feeding circuits, and high Q filters. To increase the scope of their use and to facilitate the integration with active devices, RWGs are often employed in combination with printed circuit boards (PCBs), thus leading to the integration of heterogeneous high-performance microwave or millimeter-wave systems. In this context, transitions from waveguide to planar transmission lines (e.g., microstrip lines or striplines) play a crucial role in avoiding performance degradation due to high-frequency interconnection losses.

With the emergence of millimeter-wave applications such as 5G or satellite communication, a high number of waveguide-to-PCB transitions have been proposed in the literature. In typical configurations like the ones in [1] and [2], the waveguide is orthogonally connected to the microstrip ground plane. The transitions presented in both these works have broadband responses, but an additional short-circuited quarter-wavelength waveguide section is needed on the backside of the PCB to ensure proper operation. More recently, configurations, where the presence of the back-short was avoided, have been proposed by employing a gap-coupled parasitic patch antenna as a waveguide launcher [3]. However, these transitions require a complex 3-D housing (made of brass) to be placed on top of the PCB as reported also in [4]–[6]. A fully integrated configuration that does not require any accessories, and manual assembly is proposed in [7]. However, a complex PCB manufacturing process is required due to the need to produce metalized vias of three different heights. Furthermore, several longitudinal configurations are available in the literature like in [8]–[16] and also in [17]–[19] where multisection impedance transformers have been used. However, the multisection transformers make these configurations bulky. As well, top-side transitions with a vertical configuration are usually preferable over longitudinal ones; in fact, in typical PCB designs, the antenna is commonly located on the back layer, parallel to the RF circuit that is perpendicularly connected to the waveguide. While the larger part of the mentioned transitions provides good performances in terms of insertion loss and bandwidth, many of them require a high degree of mechanical complexity. In addition, none of the mentioned solutions is suitable for dual-band applications.

In this letter, a novel vertical waveguide-to-microstrip self-diplexing transition [20], [21] is proposed. The solution is fully based on a standard multilayer PCB manufacturing process and does not require any matching structure in the rectangular waveguide. Unlike previous solutions, the proposed configuration can operate in a dual-band scenario. Our transition was optimized for the K/Ka frequency bands [22], [23] and it was conceived to provide good isolation between the two bands showing self-diplexing capabilities. The transition finds application in K/Ka-band satellite communication systems but its principles can be extended to any dual-band application whose frequency ranges lie within the waveguide operating bandwidth. Preliminary results of the proposed solution have been presented by Arnieri *et al.* [24]. To the best of the authors' knowledge, this is the first microstrip-to-waveguide transition presented in literature having dual-band capabilities.

II. Transition Configuration

Fig. 1 shows the configuration of the proposed dual-band transition. The structure is designed to excite the upper waveguide at two nonadjacent bands. A standard WR34 hollow waveguide (8.63 mm × 4.318 mm) is directly mounted on the top surface (Layer #1) of a four-metal-layer PCB to form an E-plane right-angle transition. Two microstrips printed on

Manuscript received 24 June 2022; accepted 18 July 2022. Date of publication 1 August 2022; date of current version 6 December 2022. This work was supported by the FLEXible Phased Array System for sat-COM Applications (FLEXCOM) Project, European Union's Horizon 2020 Research and Innovation Programme, under Grant 101004233. *(Corresponding author: Emilio Arnieri.)*

The authors are with the Millimeter-Wave Antennas and Integrated Circuits Laboratory (MAIC), DIMES-University of Calabria, 87036 Rende, Italy (e-mail: emilio.arnieri@unical.it).

Color versions of one or more figures in this letter are available at https://doi.org/10.1109/LMWC.2022.3193166.

Digital Object Identifier 10.1109/LMWC.2022.3193166

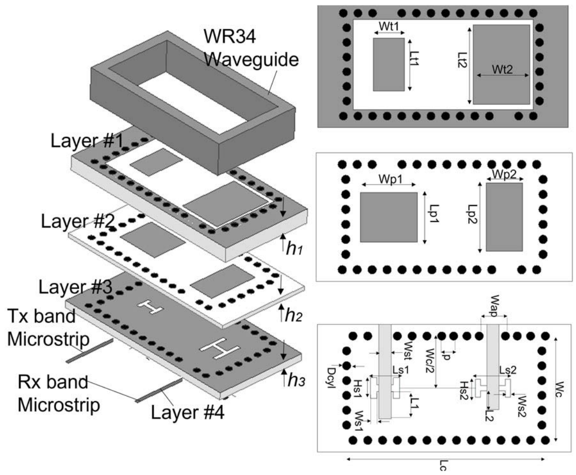

Fig. 1. Configuration of the proposed dual-band transition.

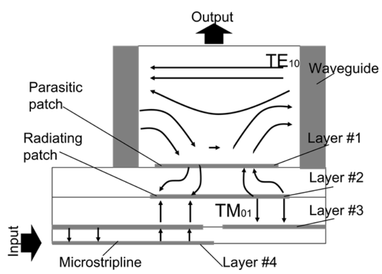

Fig. 2. Transmission mode in the proposed transition.

Layer #4 excite two patches (one for each band) placed on Layer #2 through two H-shaped slots. A parasitic patch is added on Layer #1 above each patch to widen the operating bandwidth. As demonstrated in [25], two rectangular patch antennas in a stacked configuration have a large bandwidth region which occurs when the separation between the two layers is less than 0.15λ, and a relatively high gain region is obtained if the separation exceeds 0.3λ [26]. In our case, we have separated the two patches with a 0.914-mm thin substrate ($h1 = 0.914$ mm) having Dk $= 2.33$ (see Layer #1 in Fig. 1). Separation is then $0.09\lambda 0$ at 20 GHz and $0.14\lambda 0$ at 30 GHz fulfilling the large bandwidth condition at both bands ($h1 < 0.15\lambda$).

If f_1 and f_2 are the central frequencies of the lower and upper bands, respectively, one patch is designed to resonate at f_1, while the other one at f_2. Each patch is excited by a separate feeding line. The operating principle of the transition is illustrated in Fig. 2. The quasi-TEM mode that propagates from one of the two input microstrip ports excites the TM_{01} dominant mode of the corresponding patch, thanks to the slot etched in Layer #3. The patch is sized to resonate at frequency f_1, while the stacked parasitic patch resonates at a frequency slightly different from f_1. Finally, the patch TM_{01} mode excites the TE_{10} mode of the rectangular waveguide at f_1 as illustrated in Fig. 2. The same considerations are valid for the second microstrip that excites the corresponding patch at f_2.

An SIW cavity [27], [28] has been created placing an array of metalized vias around the waveguide profile to avoid leakage from the waveguide and the excitation of traveling parallel-plate modes between the ground planes of the multilayer PCB. The size of the cavity was first estimated following [29]–[31] and then optimized with full-wave simulations [32].

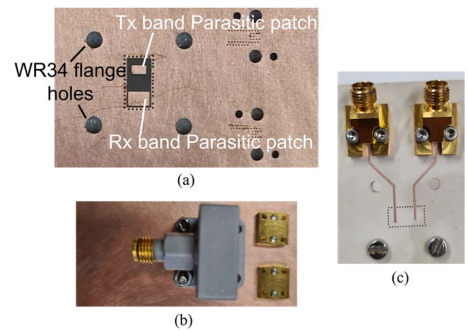

Fig. 3. Manufactured prototype of the waveguide to microstrip transition. (a) Top view. (b) Top view with connected WR34 waveguide. (c) Bottom view with mounted SMA connectors.

Rogers RT/Duroid 5870 (Dk $= 2.33$) with a thickness $h_1 = 0.914$ mm is used under Layer #1. The same material with thickness $h_2 = 0.254$ mm is used to print Layer #2. Layer #3 is printed on Rogers Ro3035 with thickness $h_3 = 0.25$ mm. A PCB fusion technique that does not require prepregs has been used to fabricate the whole stackup. Through vias are drilled from Layers #1 to #4. The proposed structure can be viewed as a cavity-backed slot antenna that excites the TE_{10} mode into the upper waveguide.

III. Simulated Performance

The physical dimensions of the two patches in Layer #2 are selected to set the resonant frequency to f_1 for one patch and f_2 for the other. Thanks to the good isolation between the two bands, parameters related to the Tx port (L1, Ls1, Hs1, Ws1, Wp1, Lp1, Wt1, and Lt1) can be optimized independent of the ones related to the Rx port (Ls2, Hs2, Ws2, Wp2, Lp2, Wt2, and Lt2). The impedance matching between the microstrips and the waveguide depends on other parameters related to the slots and parasitic patches. The transitions have been analyzed with the Ansys HFSS simulator [32]. Optimized values are (Fig. 1): $Wst = 0.58$ mm, $Wc = 4.92$ mm, $Lc = 9.23$ mm, $L1 = 0.88$ mm, $Ls1 = 1.67$ mm, $Hs1 = 0.85$ mm, $Ws1 = 0.25$ mm, $L2 = 1.30$ mm, $Ls2 = 1.39$ mm, $Hs2 = 0.98$ mm, $Ws2 = 0.31$ mm, $p = 0.7$ mm, $d = 0.4$ mm, $Wp1 = 3.05$ mm, $Lp1 = 2.17$ mm, $Wt1 = 1.54$ mm, $Lt1 = 2.54$ mm, $Wp2 = 1.60$ mm, $Lp2 = 3.62$ mm, $Wt2 = 2.50$ mm, $Lt2 = 3.75$ mm, $h1 = 0.91$ mm, $h2 = 0.25$ mm, $h3 = 0.25$ mm $d = 0.4$ mm, $p = 0.7$ mm, $Wap = 1.24$ mm, and $Dcyl = 0.4$ mm. Simulated results are presented in Section IV where simulated performances of the final configuration are compared with measurements.

IV. Experimental Results

The microstrip-to-waveguide transition has been manufactured and tested. Fig. 3 shows the fabricated prototype realized as a three-port network. Two Rosenberger 02K80F-40ML5 SMD connectors are placed on the lower side of the PCB at the end of the two microstriplines. One WR34 waveguide to coax adapter is directly screwed using its flange on the other side of the PCB. The measurement of the transmission coefficient from the waveguide to the Tx port is performed by closing

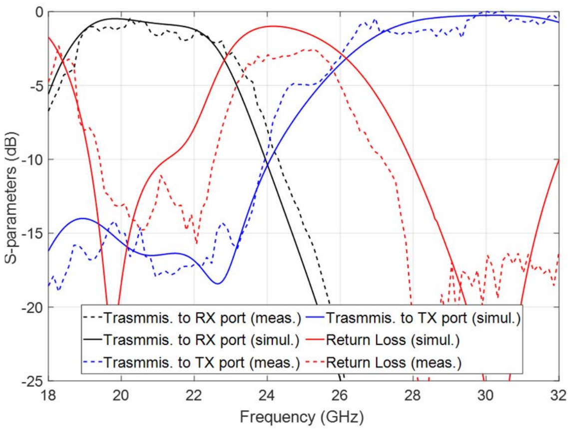

Fig. 4. Measured (dashed line) and simulated (continuous line) S-parameters.

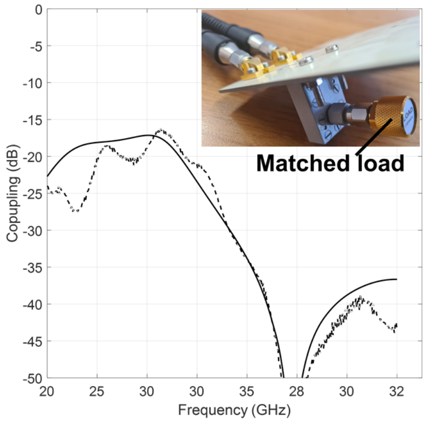

Fig. 5. Measured (dashed line) and simulated (continuous line) coupling between the two ports (Rx and Tx).

the Rx port with a matched load. Similarly, the transmission to the Tx port is performed by placing a matched load on the Rx connector. Results are visible in Fig. 4. The three-port configuration used in this prototype can be used to test the isolation between the two frequency bands. In this case, an S_{12} measurement is performed when a matched load is connected to the waveguide port. Results are shown in Fig. 5 where measurements are compared with simulation.

As it can be seen from the above figures, the measured and simulated results are in reasonable agreement except for some differences, which may be related to connectors and the PCB fabrication process. Degradation of the in-band flatness in the transmission responses is mainly related to the used waveguide to coaxial adapters. The losses of the microstrip lines were evaluated by measuring lines of different lengths obtaining a propagation loss of 0.25 dB (Rx) and 0.6 dB (Tx) for 15-mm long lines. The waveguide to coaxial adapter (VT 260WCA2.92 KPC) and the Rosenberger 02K80F-40ML5 SMD connectors have both an insertion loss of about 0.2 dB. Stripping these losses from measured S_{12}, it was found that the transition has an insertion loss of 0.6 dB in Rx and 0.7 dB in Tx. These values are the maximum insertion losses measured in the -10-dB matching bandwidth. Table I shows the performance of the dual-band transition proposed in this letter compared with state-of-the-art microstrip-to-waveguide transitions. Notice that dual-band operations are a peculiarity

TABLE I
PERFORMANCES COMPARISON

Ref.	Technology	Dual Band	Bandwidth -10dB (%)	Thick. (mm)	Max IL (dB)$^{(1)}$	Integration Level
[7]	3D Stepped SIW	No	12	0.90	0.80	High
[8]	Yagi - longitudinal	No	37	-	0.30	Low
[6]	Patch-via	No	13.8$^{(2)}$	0.16	0.41	High
[21]	SIW	No	17$^{(2)}$	0.25	1.10	High
[20]	SIW	No	6.7$^{(4)}$	0.25	>2.00	High
[28]	SIW	No	22	-	1.40$^{(5)}$	High
[33]	U-bend	No	41.8$^{(2)}$	-	0.6	Low
[34]	E-plane probe	No	27	-	0.5	Low
[35]	AMC structure	No	38	0.25	0.42	Low
[36]	E-plane probe	No	>30	1.016	2	Low
[37]	Antipodal finline	No	10	0.127	1	Low
This Work	**Multilayer PCB**	**Yes**	**20/14**	**1.41**	**0.6/0.7**	**High**

$^{(1)}$Maximum value measured in the -10dB matching bandwidth; $^{(2)}$ -15dB bandwidth; $^{(4)}$ -20dB bandwidth; $^{(5)}$ Simulation.

of the proposed solution, and for this reason, the other design included in the table are relevant to only single-band transitions. However, even considering the performance in each one of the two bands, the dual-band design compares well in terms of both bandwidth and insertion losses. A further advantage of the proposed solution is that compared to transitions included in Table I, it eases the integration in hybrid waveguide–PCB antenna designs. As an example, solutions [6] and [7] require a complex PCB manufacturing process due to the need to produce metalized vias of three different heights. Finally, configurations presented in [33] and [34] use a complex 3-D housing that requires a complex metal fabrication process.

V. CONCLUSION

In this letter, a novel vertical waveguide-to-microstrip transition for dual-band applications has been proposed. The transition provides good insertion loss and bandwidth on the two frequency ranges considered comparing well to other single-band solutions reported in the recent literature. The isolation at the two printed ports is such that the transitions can be used in a Tx/Rx antenna feeding system. The proposed transition is realized with standard PCB manufacturing processing integrated with standard waveguides, thus making it suitable for mass production and practical applications.

REFERENCES

[1] Y. Deguchi, K. Sakakibara, N. Kikuma, and H. Hirayama, "Millimeter-wave microstrip-to-waveguide transition operating over broad frequency," in *IEEE MTT-S Int. Microw. Symp. Dig.*, Jun. 2005, p. 4.

[2] Y.-C. Shih, T.-N. Ton, and L. Q. Bui, "Waveguide-to-microstrip transitions for millimeter-wave," in *IEEE MTT-S Int. Microw. Symp. Dig.*, vol. 1, May 1988, pp. 473–475.

[3] Z. Tong and A. Stelzer, "Vertical transition between rectangular waveguide and coupled microstrip lines," *IEEE Microw. Wireless Compon. Lett.*, vol. 22, no. 5, pp. 251–253, 2012.

[4] E. Topak, J. Hasch, and T. Zwick, "Compact topside millimeter-wave waveguide-to-microstrip transitions," *IEEE Microw. Wireless Compon. Lett.*, vol. 23, no. 12, pp. 641–643, Dec. 2013.

[5] A. Mozharovskiy, S. Churkin, A. Arternenko, and R. Maslcnnikov, “Wideband probe-type waveguide-to-microstrip transition for 28 GHz applications,” in *Proc. 48th Eur. Microw. Conf. (EuMC)*, Sep. 2018, pp. 113–116.

[6] N. T. Tuan, K. Sakakibara, and N. Kikuma, “Bandwidth extension of planar microstrip-to-waveguide transition by controlling transmission modes through via-hole positioning in millimeter-wave band,” *IEEE Access*, vol. 7, pp. 161385–161393, 2019.

[7] X. Dai, “An integrated millimeter-wave broadband microstrip-to-waveguide vertical transition suitable for multilayer planar circuits,” *IEEE Microw. Wireless Compon. Lett.*, vol. 26, no. 11, pp. 897–899, Nov. 2016.

[8] N. Kaneda, Y. Qian, and T. Itoh, “A broad-band microstrip-to-waveguide transition using Quasi-Yagi antenna,” *IEEE Trans. Microw. Theory Techn.*, vol. 47, no. 12, pp. 2562–2567, Dec. 1999.

[9] J. Pérez-Escudero, A. Torres-García, R. Gonzalo, and I. Ederra, “A simplified design inline microstrip-to-waveguide transition,” *Electronics*, vol. 7, no. 10, p. 215, Sep. 2018, doi: 10.3390/electronics7100215.

[10] J. M. Perez, A. Rebollo, R. Gonzalo, and I. Ederra, “An inline microstrip-to-waveguide transition operating in the full W-band based on a Chebyshev multisection transformer,” in *Proc. 10th Eur. Conf. Antennas Propag. (EuCAP)*, Apr. 2016, pp. 1–4.

[11] M. Moallem, J. East, and K. Sarabandi, “A broadband, micromachined rectangular waveguide to cavity-backed coplanar waveguide transition using impedance-taper technique,” *IEEE Trans. THz Sci. Technol.*, vol. 4, no. 1, pp. 49–55, Jan. 2014, doi: 10.1109/TTHZ.2013.2293876.

[12] Y. Lou, Q. Xue, and C. H. Chan, “A broadband waveguide-to-microstrip transition/power splitter using finline arrays,” *IEEE Microw. Wireless Compon. Lett.*, vol. 17, no. 4, pp. 310–312, Apr. 2007, doi: 10.1109/LMWC.2007.892993.

[13] J. Li, Y. Huang, Y. Li, G. Wen, and F. Xiao, “Wideband transition between rectangular waveguide and microstrip using asymmetric fin line probe,” *Electron. Lett.*, vol. 53, no. 7, pp. 490–492, Mar. 2017, doi: 10.1049/el.2016.3629.

[14] V. S. Möttönen, “Wideband coplanar waveguide-to-rectangular waveguide transition using fin-line taper,” *IEEE Microw. Wireless Compon. Lett.*, vol. 15, no. 2, pp. 119–121, Feb. 2005, doi: 10.1109/LMWC.2004.842855.

[15] V. S. Mottonen and A. V. Raisanen, “Novel wide-band coplanar waveguide-to-rectangular waveguide transition,” *IEEE Trans. Microw. Theory Techn.*, vol. 52, no. 8, pp. 1836–1842, Aug. 2004.

[16] Y. Lou, C. H. Chan, and Q. Xue, “An in-line waveguide-to-microstrip transition using radial-shaped probe,” in *Proc. IEEE Antennas Propag. Soc. Int. Symp.*, Jun. 2007, pp. 3117–3120.

[17] M. Simone, A. Fanti, G. Valente, G. Montisci, R. Ghiani, and G. Mazzarella, “A compact in-line waveguide-to-microstrip transition in the Q-band for radio astronomy applications,” *Electronics*, vol. 7, no. 2, p. 24, Feb. 2018, doi: 10.3390/electronics7020024.

[18] J. Li, L. Li, Y. Qiao, J. Chen, J. Chen, and A. Zhang, “Full Ka band waveguide-to-microstrip inline transition design,” *J. Infr., Millim., THz Waves*, vol. 39, no. 8, pp. 714–722, Aug. 2018, doi: 10.1007/s10762-018-0496-0.

[19] Y. Zhang, J. A. Ruiz-Cruz, K. A. Zaki, and A. J. Piloto, “A waveguide to microstrip inline transition with very simple modular assembly,” *IEEE Microw. Wireless Compon. Lett.*, vol. 20, no. 9, pp. 480–482, Sep. 2010, doi: 10.1109/LMWC.2010.2056358.

[20] Y. Ishikawa, K. Sakakibara, Y. Suzuki, and N. Kikuma, “Millimeter-wave topside waveguide-to-microstrip transition in multilayer substrate,” *IEEE Microw. Wireless Compon. Lett.*, vol. 28, no. 5, pp. 380–382, May 2018, doi: 10.1109/LMWC.2018.2812125.

[21] E. Hassan, M. Berggren, B. Scheiner, F. Michler, R. Weigel, and F. Lurz, “Design of planar microstrip-to-waveguide transitions using topology optimization,” in *Proc. IEEE Radio Wireless Symp. (RWS)*, Jan. 2019, pp. 1–3.

[22] Q. Luo *et al.*, “Antenna array elements for Ka-band satellite communication on the move,” in *Proc. Loughborough Antennas Propag. Conf. (LAPC)*, Nov. 2013, pp. 135–139.

[23] F. Greco, L. Boccia, E. Arnieri, and G. Amendola, “K/Ka-band cylindrical reflector antenna for compact satellite Earth terminals,” *IEEE Trans. Antennas Propag.*, vol. 67, no. 8, pp. 5662–5667, Aug. 2019, doi: 10.1109/TAP.2019.2918440.

[24] E. Arnieri, F. Greco, L. Boccia, C. Mustacchio, and G. Amendola, “Dual band topside waveguide-to-stripline transition in multilayer substrate,” in *Proc. IEEE Int. Symp. Antennas Propag. USNC-URSI Radio Sci. Meeting (APS/URSI)*, Dec. 2021, pp. 691–692, doi: 10.1109/APS/URSI47566.2021.9703769.

[25] R. Q. Lee and K.-F. Lee, “Experimental study of the two-layer electromagnetically coupled rectangular patch antenna,” *IEEE Trans. Antennas Propag.*, vol. 38, no. 8, pp. 1298–1302, Aug. 1990, doi: 10.1109/8.56971.

[26] E. Arnieri, G. Amendola, and L. Boccia, “A cavity-backed shorted annular patch (SAP) array for mid-range V-band backhauling applications,” *IEEE Access*, vol. 7, pp. 38179–38184, 2019, doi: 10.1109/ACCESS.2019.2905106.

[27] L. Boccia, A. Emanuele, E. Arnieri, A. Shamsafar, and G. Amendola, “Substrate integrated power combiners,” in *Proc. 6th Eur. Conf. Antennas Propag. (EUCAP)*, 2012, pp. 3631–3634, doi: 10.1109/EuCAP.2012.6206405.

[28] H. A. Diawuo and Y.-B. Jung, “Waveguide-to-stripline transition design in millimeter-wave band for 5G mobile communication,” *IEEE Trans. Antennas Propag.*, vol. 66, no. 10, pp. 5586–5589, Oct. 2018, doi: 10.1109/TAP.2018.2854364.

[29] E. Abaei, E. Mehrshahi, G. Amendola, E. Arnieri, and A. Shamsafar, “Two dimensional multi-port method for analysis of propagation characteristics of substrate integrated waveguide,” *Prog. Electromagn. Res. C*, vol. 29, pp. 261–273, 2012, doi: 10.2528/PIERC12022506.

[30] G. Amendola, G. Angiulli, E. Arnieri, and L. Boccia, “Computation of the resonant frequency and quality factor of lossy substrate integrated waveguide resonators by method of moments,” *Prog. Electromagn. Res. Lett.*, vol. 40, pp. 107–117, 2013, doi: 10.2528/PIERL13031808.

[31] G. Angiulli, E. Arnieri, D. D. Carlo, and G. Amendola, “Fast nonlinear eigenvalues analysis of arbitrarily shaped substrate integrated waveguide (SIW) resonators,” *IEEE Trans. Magn.*, vol. 45, no. 3, pp. 1412–1415, Mar. 2009, doi: 10.1109/TMAG.2009.2012650.

[32] (Jun. 25, 2019). *High Frequency Surface Structure (HFSS) (19 ed.)*. [Online]. Available: http://www.ansys.com

[33] C. Wu *et al.*, “Millimeter-wave waveguide-to-microstrip inline transition using a wedge-waveguide iris,” *IEEE Trans. Microw. Theory Techn.*, vol. 70, no. 2, pp. 1087–1096, Nov. 2021.

[34] Z. Xu, J. Xu, and C. Qian, “Novel in-line microstrip-to-waveguide transition based on E-plane probe T-junction structure,” *IEEE Microw. Wireless Compon. Lett.*, vol. 31, no. 9, pp. 1051–1054, Sep. 2021.

[35] A. U. Zaman, V. Vassilev, P.-S. Kildal, and H. Zirath, “Millimeter wave E-plane transition from waveguide to microstrip line with large substrate size related to MMIC integration,” *IEEE Microw. Wireless Compon. Lett.*, vol. 26, no. 7, pp. 481–483, Jul. 2016, doi: 10.1109/LMWC.2016.2574995.

[36] E. S. Li, G.-X. Tong, and D. C. Niu, “Full W-band waveguide-to-microstrip transition with new E-plane probe,” *IEEE Microw. Wireless Compon. Lett.*, vol. 23, no. 1, pp. 4–6, Jan. 2013, doi: 10.1109/LMWC.2012.2235176.

[37] S. Jing, L. Fa-Guo, H. Li-Hua, and S. Xiao-Ying, “Waveguide-to-microstrip antipodal finline transition at W band,” in *Proc. 3rd Int. Conf. Instrum., Meas., Comput., Commun. Control*, Sep. 2013, pp. 510–513, doi: 10.1109/IMCCC.2013.116.

Open Access funding provided by ‘Università della Calabria’ within the CRUI CARE Agreement